Tree simplification and the 'plateaux' phenomenon of graph Laplacian eigenvalues

Naoki Saito[a,*], Ernest Woei[a,1]

[a]*Department of Mathematics, University of California, Davis, CA 95616, USA*

Abstract

We developed a procedure of reducing the number of vertices and edges of a given tree, which we call the "tree simplification procedure," without changing its topological information. Our motivation for developing this procedure was to reduce computational costs of graph Laplacian eigenvalues of such trees. When we applied this procedure to a set of trees representing dendritic structures of retinal ganglion cells of a mouse and computed their graph Laplacian eigenvalues, we observed two "plateaux" (i.e., two sets of multiple eigenvalues) in the eigenvalue distribution of each such simplified tree. In this article, after describing our tree simplification procedure, we analyze why such eigenvalue plateaux occur in a simplified tree; explain such plateaux can occur in a more general graph if it satisfies a certain condition; and identify these two eigenvalues specifically as well as the lower bound to their multiplicity.

Keywords: vertex reduction; graph Laplacian eigenvalues; eigenvalue multiplicity; monic polynomials with integer coefficients
2000 MSC: 05C07, 05C50, 15A42, 65F15

1. Introduction

In order to characterize and cluster dendritic trees of retinal ganglion cells (RGCs) of a mouse, our previous work [9] illustrated the use of graph Laplacian eigenvalues rather than using the morphological features derived manually from those dendritic trees. We note that each dendritic tree was literarily

*Corresponding author
Email addresses: saito@math.ucdavis.edu (Naoki Saito), woei@math.ucdavis.edu (Ernest Woei)
[1]Currently at: FlashFoto, Inc., Los Gatos, CA 95030, USA.

represented by a tree in the sense of graph theory. Furthermore, in [10, 8], we provided our theoretical understanding of the peculiar eigenvalue/eigenvector phase transition phenomenon we observed on each of our dendritic trees.

Continuing on our road to characterizing dendritic trees, once more we observed a new eigenvalue phenomenon on our simplified (or vertex-subsampled) dendritic trees. Discovery of this phenomenon has the following history. Each of the dendritic trees first analyzed in [9] has a large number of vertices (ranging from 565 to 24474 depending on the RGCs) since they represent dense spatial sample points traced along the actual dendritic arbors in the 3D images measured by a confocal microscope using specialized segmentation software operated by our neuroscience collaborators; see [3] for the details. If we are only concerned about their *topological* properties (e.g., connectivities of various branches, bifurcation patterns, etc.) but not their *geometric aspects* (e.g., branch lengths, branch angles, etc.), then it is unnecessary to keep most of the vertices of degree 2 since they do not alter topology of the trees. Section 3 describes our procedure to eliminate such vertices, which we call a "tree simplification procedure." After simplifying all these trees, we once again started analyzing their graph Laplacian eigenvalues. Interestingly enough, the phase transition phenomenon we observed in the original trees disappeared completely. Instead, we observed a new phenomenon in the eigenvalue distributions of such simplified trees. For each such simplified tree, the eigenvalue distribution has two "plateaux," i.e., a pair of distinct eigenvalues having the same multiplicity greater than one as shown in Figures 6 and 7. The purpose of this article is to describe this phenomenon and provide a theoretical explanation of this phenomenon.

The organization of this article is the following. Section 2 sets up our notation for this article and defines some basic quantities. Then, Section 3 describes our tree simplification procedure and illustrates several examples. Section 4 describes our main result along with its theoretical consequences. Finally, we conclude in Section 5 with discussion and state a conjecture on more general situations.

2. Notation and Definitions

In this article, we follow the standard notation and terminology in the graph theory literature, e.g., [6]. All the graphs we consider throughout are finite, simple (i.e., with no multiple, weighted, or directed edges and no loops), and connected. Let $G = (V, E)$ be a graph where $V = V(G) = \{v_1, v_2, \ldots, v_n\}$ is the *vertex*

set of G and $E = E(G) = \{e_1, e_2, \ldots, e_m\}$ is its *edge set* where e_k connects two vertices v_i, v_j for some $1 \leq i \neq j \leq n$. $|V| = n$ is also referred to as the *order* of V. The *degree* of a vertex v, i.e., the number of edges incident with v, is denoted as d_v. A vertex v is referred to as a *leaf* or a *pendant vertex* if $d_v = 1$. A *path* from v_i to v_j in a graph G is a subgraph of G consisting of a sequence of distinct vertices starting with v_i and ending with v_j such that consecutive vertices are adjacent. We say the *length* $\ell(P)$ of a path P is the number of its edges, i.e., $\ell(P) := |E(P)|$. A *rooted tree* $T(V, E)$ is a tree with a vertex labeled as the *root* vertex, $v_r \in V$. A *starlike* tree is a tree which has exactly one vertex of degree greater than 2. Let $S(n_1, n_2, \ldots, n_k)$ be a starlike tree that has $k(\geq 3)$ paths (i.e., branches) emanating from the central vertex v_1 with $d_{v_1} = k$. Let the ith branch have n_i vertices excluding v_1. Let $n_1 \geq n_2 \geq \cdots \geq n_k$. Then, $n = |V(S(n_1, \ldots, n_k))| = 1 + \sum_{i=1}^{k} n_i$.

In this article, we refer to a vertex of degree 2 in a given graph as a *trivial* vertex. All the other vertices are referred to as *nontrivial*, with the following exception: if the graph is a rooted tree, then its root vertex is treated as a nontrivial vertex regardless of its degree. For a graph $G(V, E)$, a pair of nontrivial vertices, say, $(v_{i_1}, v_{i_k}) \in V \times V$, is referred to as a *neighboring pair of nontrivial vertices* if there is a path between them with a vertex sequence $\left(v_{i_1}, v_{i_2}, \ldots, v_{i_k}\right)$ where the intermediate vertices $v_{i_2}, \ldots, v_{i_{k-1}}$ are all trivial.

The *Laplacian matrix* of G is $L(G) := D(G) - A(G)$ where $A(G) = \left(a_{ij}\right)$ and $D(G) := \operatorname{diag}\left(d_{v_1}, \ldots, d_{v_n}\right)$ are the *adjacency matrix* and the *degree matrix* of G, respectively. Let $0 = \lambda_0 \leq \lambda_1 \leq \cdots \leq \lambda_{n-1}$ be the sorted eigenvalues of $L(G)$. Let $m_G(\lambda)$ denote the multiplicity of the eigenvalue λ of $L(G)$, and let $m_G(I)$ be the number of eigenvalues of $L(G)$, multiplicities included, that belong to I, an interval of the real line.

3. Tree Simplification

As mentioned earlier, we only deal with *simple, connected, undirected, and unweighted* graphs in this article as we did in our previous works [9, 10, 8]. In other words, we focus on the topological aspects of graphs rather than geometrical aspects. For the latter, we refer the readers to [13, Chap. 7] as well as our ongoing work [2]. We also assume that each tree we deal with in this article is a rooted tree whose root vertex corresponds to the so-called "soma" (a.k.a. cell body) if that tree represents an actual neuronal dendritic tree. Once we decide to restrict our attention to the topological aspects of trees, then it seems obvious that all trivial vertices defined earlier can be removed without altering the topology and connectivities. Removal of such trivial vertices certainly

saves subsequent computations of eigenvalues and eigenvectors of the resulting Laplacian matrices.

Can we really remove all trivial vertices in an original tree? If we dealt with topological and geometrical aspects of trees by using weighted trees with edge weight representing the Euclidean distance between the associated pair of vertices, then the answer would be 'Yes'. However, the answer is in fact 'No' for unweighted trees of our interest. This is due to the existence of the so-called *spines*[2] in our dendritic trees. Each spine is represented by a *pendant edge* (i.e., an edge connecting a leaf and one of the intermediate vertices in a path); see, e.g., Figure 5.

We want to distinguish spines from longer paths in our resulting simplified trees. To do so, we need to do the following: for each pair of *neighboring* nontrivial vertices in an original tree, check the length of its associated path; if it is greater than one (i.e., a non-spine path), then we remove all those intermediate trivial vertices but one in the middle of the path, which results in the path of length two. Note that this tree simplification procedure keeps all the spines intact.

Let us briefly illustrate the benefits we obtain from this tree simplification procedure on our dataset by displaying a histogram of an agglomeration of all the vertices and their degrees over all dendritic trees in Figure 1(a). There we can see that the number of trivial vertices outnumber the number of nontrivial vertices. Most trivial vertices in our original dendritic trees lie on paths between neighboring nontrivial vertices. Figure 1(b) shows the degree distribution of the simplified dendritic trees after our tree simplification procedure is applied. We can see that the number of degree 2 vertices in the simplified trees are comparable with the nontrivial vertices with degree 1 and degree 3. See also Table 1 for more quantitative information on our tree simplification procedure applied to our dendritic trees.

Let us now describe our tree simplification procedure in detail. Let $T(V,E)$ be a rooted tree. Assume V is an ordered list of vertices that are labeled as v_i for $i = 1,\ldots,n = |V|$. Without loss of generality, let us assume v_1 is the labeled root vertex. Our procedure starts by examining vertex v_1, then v_2, and so on till we examine the last vertex v_n (See Algorithm 1).

[2]Spines are small membranous protrusion along a neuron's dendrite. They typically receive input from a single synapse of another neuron's axon. They also serve as a storage site for synaptic strength and help transmit electrical signals to the neuron's cell body [12]. Therefore, spines are a very important feature of dendrites.

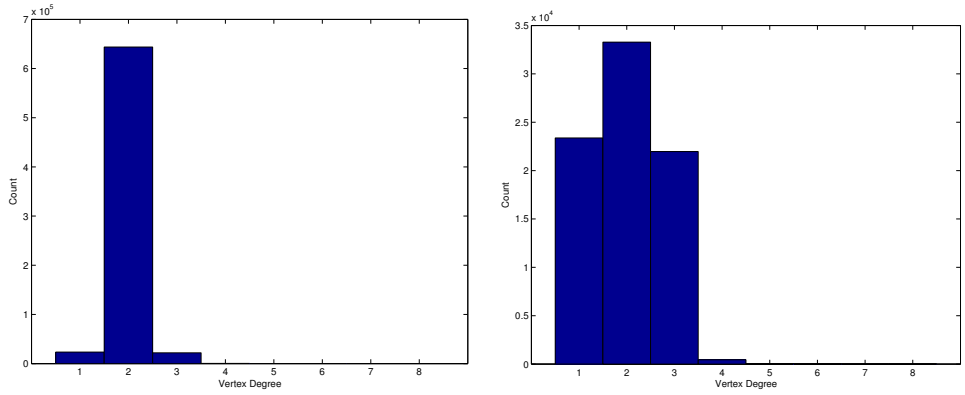

(a) (b)

Figure 1: Histogram of an agglomeration of all vertices and their degrees for (a) unmodified dendritic trees; (b) simplified dendritic trees with one trivial vertex on each non-spine path. Note that the scale of the vertical axis in (a) is different from that in (b).

Algorithm 1 Tree Simplification

1: Set $i = 0$.
2: If $i > n$, then terminate; else set $i = i + 1$ and $v = v_i$.
3: If v is v_1 or $v \notin V$, then goto **Step 2**.
4: If $d_v \neq 2$, then goto **Step 2**.
5: If $d_v = 2$, then v is adjacent to two vertices. Let u and w be these two vertices. If u or w is v_1, then goto **Step 2**.
6: If $d_u = 2$, then 'coalesce' u and v (i.e., delete the edges (v,u), (v,w) from E; add a new edge (u,w) to E; and delete v from V), and goto **Step 2**.
7: If $d_w = 2$, then follow **Step 6** with w instead of u.
8: Go to **Step 2**.

A few remarks are in order. First, note that from **Step 3** to **Step 7**, we would coalesce *at most* one pair of vertices. Second, upon the completion of the above procedure, the pair of sets (V,E) form the desired simplified tree. The number of nontrivial vertices in the simplified tree is preserved by this simplification procedure as can be seen from **Step 3** and **Step 4**.

Now let us illustrate our tree simplification procedure by applying it to very simple two trees in Figures 2 and 3. Figure 2 shows a simplification of tree P_6 with root vertex v_r to P_4. In Figure 3, the tree simplification procedure keeps P_5 intact since v_r is adjacent to two trivial vertices, hence we "go back" to **Step 2**

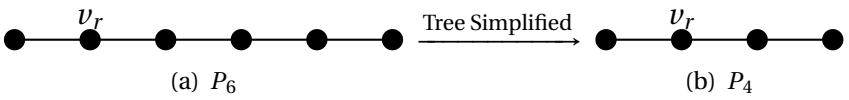

Figure 2: P_6 simplified to P_4.

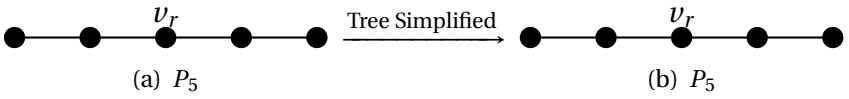

Figure 3: P_5 with center root vertex simplified is still P_5.

in **Steps 3** and **5**.

Figures 4 and 5 illustrate the simplified trees of a few dendritic trees in our dataset. Table 1 provides information about how much we simplified (i.e., subsampled) our original dendritic trees. From this table, we see that on average, approximately 84% of vertices of our dendritic trees are removed by our procedure.

4. Eigenvalue 'Plateaux' Phenomenon

After simplifying all of the dendritic trees in our dataset, we computed their Laplacian eigenvalues. We then observed an "eigenvalue plateaux" phenomenon for each of the newly formed simplified trees. In Figures 6 and 7, we display a couple of simplified trees and their respective eigenvalue plots. The eigenvalues which form these plateaux are approximately 0.3820 and 2.6180. In fact, as we will explain shortly, these values are more precisely written as $\theta := \frac{3-\sqrt{5}}{2} = 2-2\cos\frac{\pi}{5} \approx 0.3820$ and $\theta^* := \frac{3+\sqrt{5}}{2} = 2-2\cos\frac{3\pi}{5} \approx 2.6180$. It is interesting to note that the multiplicity of each of those eigenvalues are exactly the same. In Table 2, we present some statistical information on the eigenvalue multiplicity across all trees for each cluster. For these dendritic trees, the multiplicities of θ were determined numerically by counting all the eigenvalues lying within the interval of width of 2×10^{-10} centered at θ, and the same procedure was used for θ^*.

Below we mention a simple example of a tree which contains these eigenvalues and a type of tree that has identical multiplicities of θ and θ^*.

Example 4.1. The simplest tree possessing Laplacian eigenvalues θ and θ^* is P_5. It is well known that the eigenvalues of P_n are $2-2\cos\frac{k\pi}{n}$ for $k = 0,1,\ldots,n-1$; see, e.g., [11]. Hence for $n = 5$, we have $\theta = 2-2\cos\frac{\pi}{5}$ and $\theta^* = 2-2\cos\frac{3\pi}{5}$.

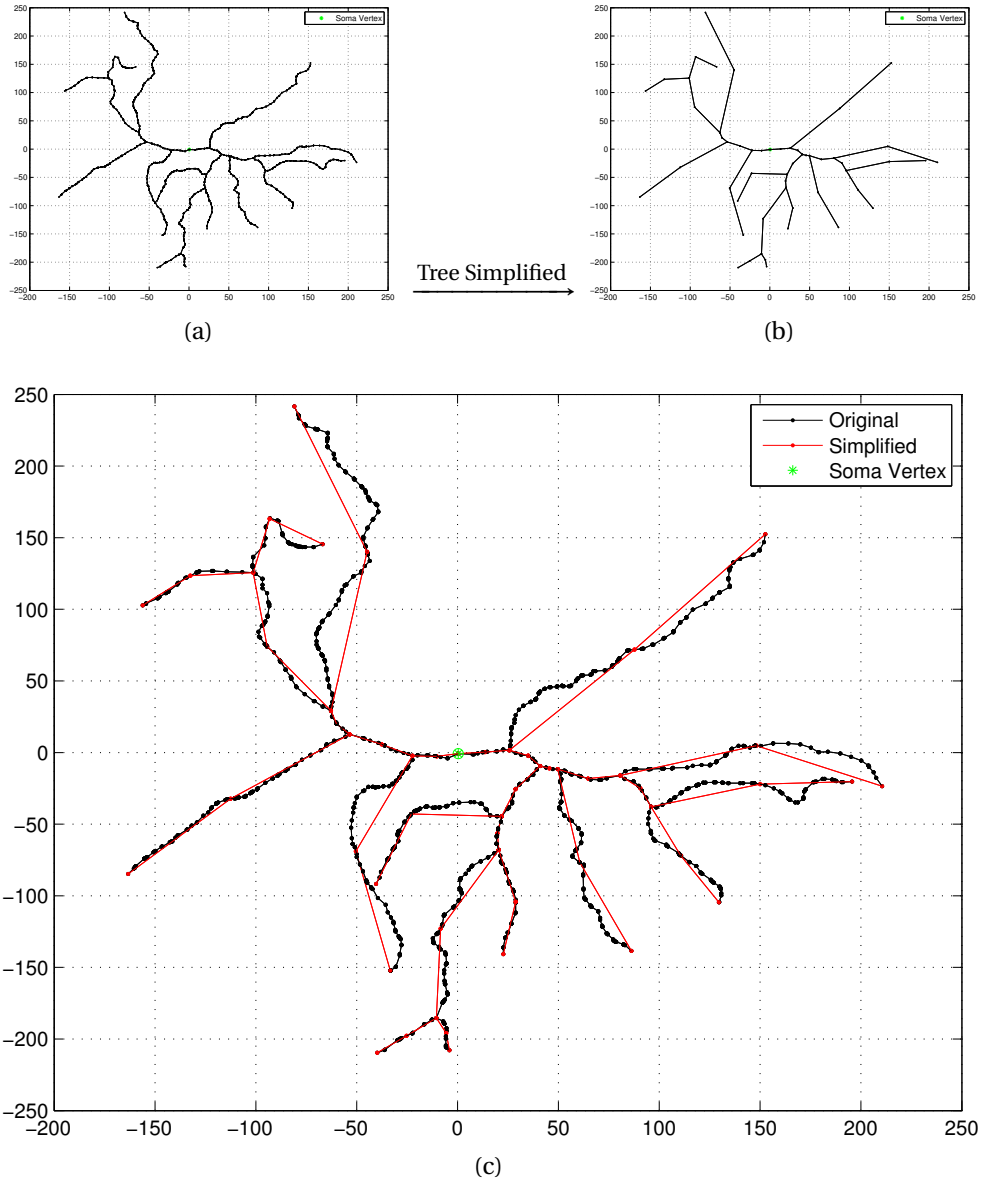

Figure 4: RGC #100 from Cluster 6. (a) Original, 1154 vertices. (b) Simplified, 53 vertices. (c) Overlayed. Approximately 95% vertices reduction from the original tree to the simplified tree. Note that these plots are 2D projections of the 3D dendritic structures since each original vertex has a 3D spatial coordinate. The units of the horizontal and vertical axes are in μm = 10^{-6}meter.

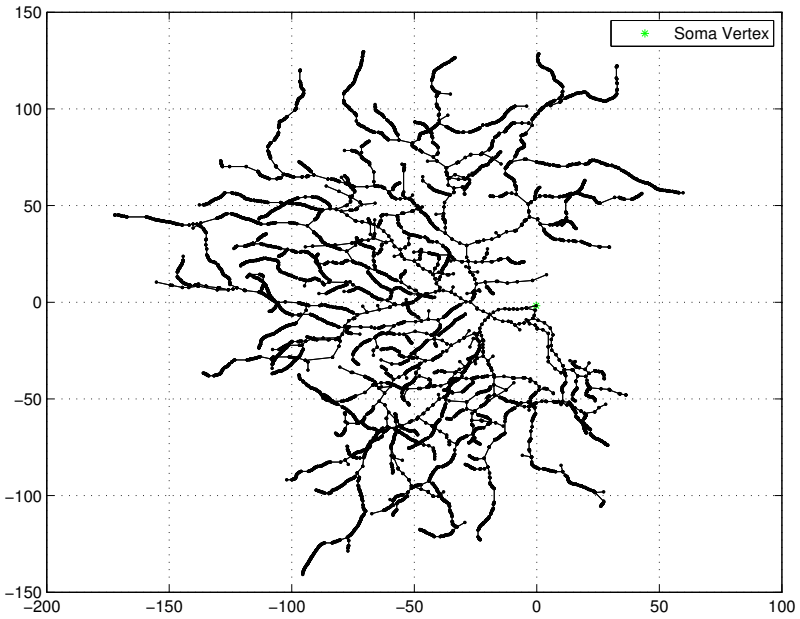

(a)

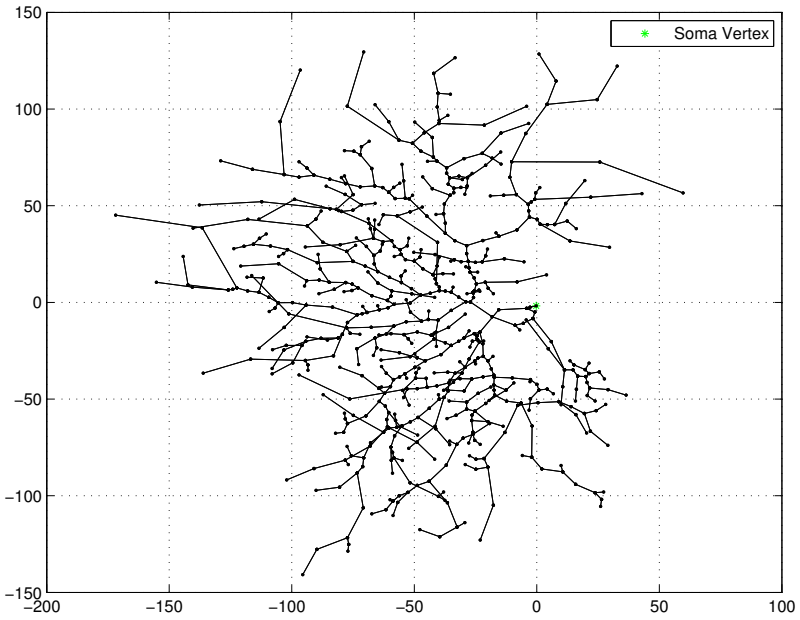

(b)

Figure 5: RGC #60 from Cluster 1. (a) Original, 5636 vertices. (b) Simplified, 612 vertices. Approximately 89% vertices reduction from the original tree to the simplified tree. Note that "spines" are preserved.

Vertex Count Statistical Information							
Cluster #	# RGCs	$\overline{\lvert V_o \rvert}$	σ_o	$\overline{\lvert V_s \rvert}$	σ_s	Red. Avg.	Red. Std.
1	9	4650.8	3693.68	866.8	189.98	70.23%	17.80%
2	8	1562.4	565.18	337.1	167.65	78.46%	5.78%
3	18	2262.4	1448.48	422.7	169.37	77.83%	8.27%
4	8	9378.1	7369.27	645.0	300.54	88.38%	8.50%
5	10	2778.1	1841.34	343.6	115.20	85.02%	6.68%
6	9	758.7	172.16	39.6	19.60	94.55%	3.11%
7	15	3245.0	3299.06	333.3	52.40	83.44%	8.46%
8	19	3323.5	2125.14	302.7	49.42	87.25%	6.81%
9	21	3113.9	2021.73	210.7	60.25	90.23%	6.21%
10	13	3561.8	2727.46	173.6	35.98	91.22%	6.18%
11	12	4668.8	2697.87	981.7	256.64	74.53%	10.95%
12	9	8273.1	6809.86	599.3	189.34	87.02%	10.89%
13	19	5043.2	2744.18	724.8	205.49	80.62%	11.56%
14	8	3684.0	2763.62	446.9	144.29	83.49%	7.10%
no	1	5590.0	0.00	103.0	0.00	98.16%	0.00%
Total	179	3852.5	3565.28	442.0	293.10	83.99%	10.89%

Table 1: Vertex count statistical information for the original and simplified dendritic trees for each cluster of RGCs. These clusters were identified by Coombs et al. [3] from their morphological analysis followed by the hierarchical clustering technique. Cluster 'no' indicates a singular dendritic tree that does not belong to any of the 14 distinct clusters. The 3rd and 5th columns are the *average* number of vertices across all trees for each cluster, for the original and simplified tree, respectively. The 4th and 6th columns represent the *standard deviation* of the number of vertices across all trees for each cluster. The final two columns represent the *average percentage reduction* and *reduction standard deviation* of number of vertices from the original to the simplified dendritic tree. The subscripts 'o' and 's' indicate 'original' and 'simplified', respectively.

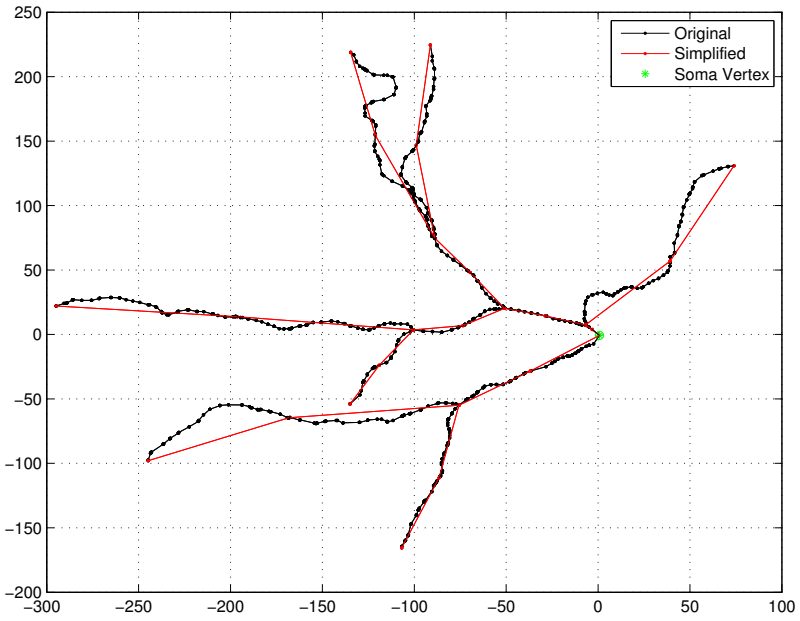

(a)

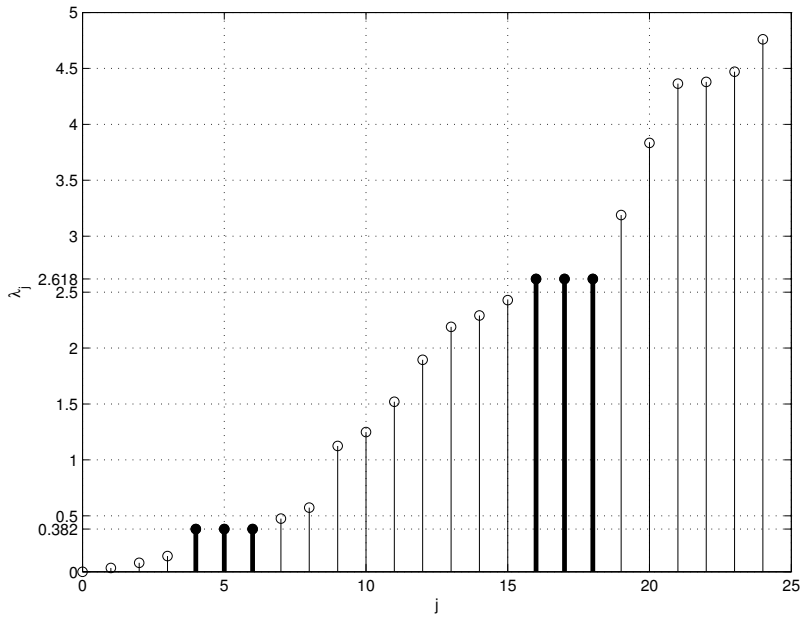

(b)

Figure 6: RGC #102 of Cluster 6. (a) Simplified tree overlaid on original dendritic tree. (b) Eigenvalue distribution of the simplified tree. Note that $m_T(\theta) = m_T(\theta^*) = 3$.

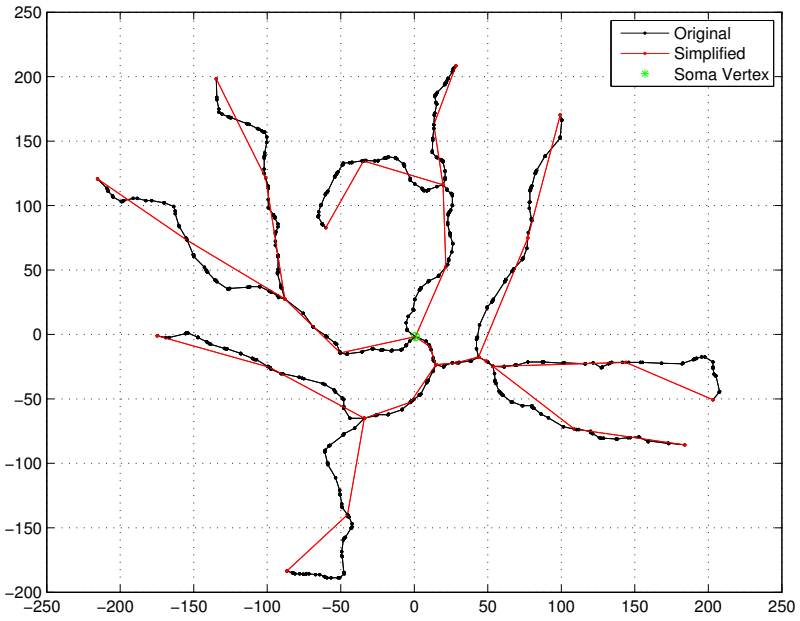

(a)

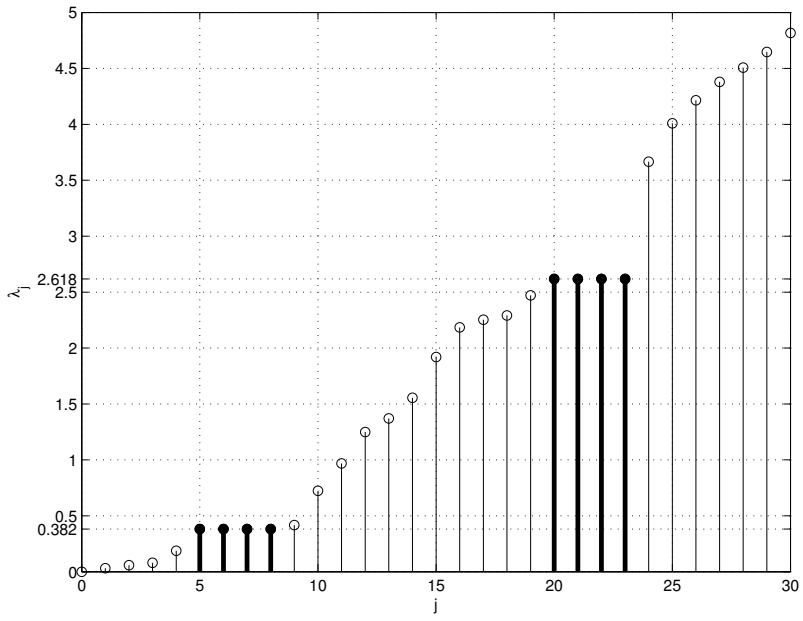

(b)

Figure 7: RGC #108 of Cluster 6. (a) Simplified tree overlaid on original dendritic tree. (b) Eigenvalue distribution of the simplified tree. Note that $m_T(\theta) = m_T(\theta^*) = 4$.

Eigenvalue Multiplicity Statistical Information					
Cluster #	$\overline{m_T(\{\theta,\theta^*\})}$	σ_m	Cluster #	$\overline{m_T(\{\theta,\theta^*\})}$	σ_m
1	29.3	15.94	2	20.2	10.27
3	34.2	11.45	4	58.8	19.54
5	24.8	11.43	6	7.6	3.98
7	36.3	10.19	8	31.2	8.47
9	26.3	6.85	10	20.8	9.43
11	68.7	39.04	12	36.7	10.99
13	34.6	9.99	14	34.0	8.25
no	20.0	0.00	All	32.9	19.61

Table 2: Summary of the Laplacian eigenvalue multiplicity of the simplified dendritic trees of our dataset separated by each cluster. The 2nd and 5th columns contain the *average multiplicity* of the eigenvalues θ and θ^*, while the 3rd and 6th columns contain the *standard deviation* of these specific eigenvalue multiplicities. Note that $\overline{m_T(\{\theta,\theta^*\})} = 2m_T(\theta) = 2m_T(\theta^*)$.

Now the following proposition demonstrates a concrete example of the existence of θ and θ^* with multiplicities.

Proposition 4.2. *Let* $T(V,E) = S(k.2) := S(\underbrace{2,2,\ldots,2}_{k})$ *be a starlike tree with* $k > 1$ *branches with each branch containing 2 vertices so that* $|V| = 2k+1$. *Then* $m_T(\theta) = m_T(\theta^*) = k-1$.

We note that $P_5 = S(2.2)$.

Proof. This easily follows from the following lemma due to Das:

Lemma 4.3 (See Das [4, Lemma 3.1])**.** *The Laplacian eigenvalues of starlike tree* $S(k.m)$ *are*

$$2+2\cos\Big(\frac{p\pi}{2m+1}\Big), \quad p = 2,4,\ldots,2m, \tag{1}$$

and each of multiplicity $k-1$. *Also the remaining eigenvalues satisfy the following system of equations:*

$$\begin{cases} \lambda x_1 = x_1 - x_2 \\ \lambda x_i = 2x_i - x_{i-1} - x_{i+1} \quad i = 2,3,\ldots,m \\ \lambda x_{m+1} = kx_{m+1} - kx_m \end{cases}$$

Hence, setting $m = 2$ in this lemma, the eigenvalues (1) are of the form $2 + 2\cos\frac{p\pi}{5}$, $p = 2, 4$. But $2+2\cos\frac{2\pi}{5} = 2-2\cos\frac{3\pi}{5} = \theta^*$, and $2+2\cos\frac{4\pi}{5} = 2-2\cos\frac{\pi}{5} = \theta$. Their multiplicities are $k-1$ as Das's lemma guarantees. □

We now explain why the eigenvalue plateaux phenomenon occurs in our simplified dendritic trees. First, let us define some notation that will be used in our theorem below. Let $G(V, E)$ be a simple, connected, undirected, and unweighted graph. Let

$$V_1 := \{v \in V \mid d_v = 1\} \subset V \tag{2}$$

be the set of *pendant vertices* and

$$V_{2\sim 1} := \{v \in V \mid d_v = 2 \text{ and } \exists u \in V_1 \text{ s.t. } u \sim v\} \tag{3}$$

be the set of *pendant neighbors of degree 2*, and

$$V_I := \{v \in V \mid d_v \geq 3 \text{ and } \exists u \in V_{2\sim 1} \text{ s.t. } u \sim v\} \tag{4}$$

be the set of *vertices of degree 3 or greater which are adjacent to vertices in* $V_{2\sim 1}$. For every $v \in V_I$, let us define the following two quantities

$$c(v) := \left|\left\{v' \in V_{2\sim 1} \mid v' \sim v\right\}\right| \tag{5}$$

and

$$\tau_{V_I} := \sum_{v \in V_I} (c(v) - 1)\,. \tag{6}$$

Note that there may be vertices of degree 3 or greater in V that do not belong to V_I. The following theorem explains the eigenvalue plateaux phenomenon *not only for simplified trees but also for more general graphs.*

Theorem 4.4. *Let $G(V, E)$ be a simple, connected, undirected, and unweighted graph with $n = |V|$. Let $\theta = \frac{3-\sqrt{5}}{2}$ and $\theta^* = \frac{3+\sqrt{5}}{2}$ be as defined previously in this section. Suppose $\tau_{V_I} \geq 1$, then*

$$m_G(\theta) = m_G(\theta^*) \geq \tau_{V_I}\,. \tag{7}$$

In other words, the multiplicity of the graph Laplacian eigenvalues θ and that of θ^* are the same and at least τ_{V_I}.

Proof. Let $\kappa := |V_I|$. If $\kappa = 0$, then obviously $\tau_{V_I} = 0 \le m_G(\theta)$. Similarly, for $m_G(\theta^*)$. Suppose $\kappa > 0$, then $V_I \neq \emptyset$. For every $v \in V_I$, we have $c(v) \ge 1$ by the definitions of (5) and (4).

Suppose $V_I = \{v_1, \ldots, v_\kappa\}$. A Laplacian matrix of G takes the form

$$L(G) = \left[\begin{array}{ccc|ccc|c} B_1 & & & \boldsymbol{r}_1 & & & \\ & \ddots & & & \ddots & & \\ & & B_\kappa & & & \boldsymbol{r}_\kappa & \\ \hline \boldsymbol{r}_1^\mathsf{T} & & & & & & \\ & \ddots & & & C_1 & & C_2 \\ & & \boldsymbol{r}_\kappa^\mathsf{T} & & & & \\ \hline & & & & & & \\ & & & & C_3 & & C_4 \\ & & & & & & \end{array}\right], \tag{8}$$

where for each j with $1 \le j \le \kappa$, and $B_j := \operatorname{diag}(Q, \ldots, Q) \in \mathbb{R}^{2c(v_j) \times 2c(v_j)}$, i.e., a block diagonal matrix with $c(v_j)$ copies of $Q := \begin{bmatrix} 2 & -1 \\ -1 & 1 \end{bmatrix}$, and $\boldsymbol{r}_j \in \mathbb{R}^{2c(v_j) \times 1}$ is a vector of $c(v_j)$ stacks of the vector $\boldsymbol{r} := \begin{bmatrix} -1 \\ 0 \end{bmatrix}$, i.e.,

$$\boldsymbol{r}_j := \begin{bmatrix} \boldsymbol{r} \\ \boldsymbol{r} \\ \vdots \\ \boldsymbol{r} \end{bmatrix} \in \mathbb{R}^{2c(v_j) \times 1}.$$

Note that the eigenvalues of Q is θ and θ^*.

To describe the block matrices C_ℓ for $\ell = 1, 2, 3, 4$, first let us define

$$V_{2\sim 1}^I := \left\{ v \in V_{2\sim 1} \,|\, \exists v' \in V_I \text{ s.t. } v \sim v' \right\} \subseteq V_{2\sim 1} \tag{9}$$

and

$$V_1^I := \left\{ v \in V_1 \,|\, \exists v' \in V_{2\sim 1}^I \text{ s.t. } v \sim v' \right\} \subseteq V_1. \tag{10}$$

Note that $\left|V_{2\sim 1}^I\right| = \left|V_1^I\right| = \sum_{j=1}^{\kappa} c(v_j)$. Let $V_r := V \setminus \left(V_I \cup V_{2\sim 1}^I \cup V_1^I\right)$. C_1 is a $\kappa \times \kappa$ matrix whose diagonal entries are $d_{v_1}, d_{v_2}, \ldots, d_{v_\kappa}$ and whose off-diagonal entries depends on the interactions (edges) between vertices within V_I. The block matrices C_2 and C_3 correspond to the interactions between vertices in V_I and

V_r, while the block matrix C_4 corresponds to the interactions between vertices within V_r.

We need only consider the case when $c(v_j) > 1$, since if $c(v_j) = 1$, then it does not contribute to the sum in (6). Our strategy is to construct a set of $c(v_j) - 1$ eigenvector(s) associated with the eigenvalue λ, where $\lambda = \theta$ or θ^* or equivalently when λ satisfies the characteristic equation $\lambda^2 - 3\lambda + 1 = 0$. First, let

$$\boldsymbol{x}_\lambda := \begin{bmatrix} \frac{-1}{2-\lambda} \\ -1 \end{bmatrix} \tag{11}$$

and let $\mathbf{0}_k$ denote the zero vector of length k.

For $\ell = 1, \ldots, c(v_j)-1$, let $\boldsymbol{y}_\ell$ be the vector of length $2c(v_j)$ where $\boldsymbol{x}_\lambda$ occupies the 1st and 2nd entries of $\boldsymbol{y}_\ell$ and $-\boldsymbol{x}_\lambda$ occupies the $2\ell+1$ and $2\ell+2$ entries of $\boldsymbol{y}_\ell$, i.e.,

$$\boldsymbol{y}_\ell = \begin{bmatrix} \boldsymbol{x}_\lambda \\ \mathbf{0}_2 \\ \vdots \\ \mathbf{0}_2 \\ -\boldsymbol{x}_\lambda \\ \mathbf{0}_2 \\ \vdots \\ \mathbf{0}_2 \end{bmatrix} \leftarrow 2\ell+1 \text{ and } 2\ell+2 \text{ positions.}$$

Therefore,

$$\boldsymbol{y}_\ell \in \underbrace{\left\{ \begin{bmatrix} \boldsymbol{x}_\lambda \\ -\boldsymbol{x}_\lambda \\ \mathbf{0}_2 \\ \vdots \\ \vdots \\ \vdots \\ \mathbf{0}_2 \end{bmatrix}, \begin{bmatrix} \boldsymbol{x}_\lambda \\ \mathbf{0}_2 \\ -\boldsymbol{x}_\lambda \\ \mathbf{0}_2 \\ \vdots \\ \vdots \\ \mathbf{0}_2 \end{bmatrix}, \ldots, \begin{bmatrix} \boldsymbol{x}_\lambda \\ \mathbf{0}_2 \\ \vdots \\ \vdots \\ \mathbf{0}_2 \\ -\boldsymbol{x}_\lambda \\ \mathbf{0}_2 \end{bmatrix}, \begin{bmatrix} \boldsymbol{x}_\lambda \\ \mathbf{0}_2 \\ \vdots \\ \vdots \\ \mathbf{0}_2 \\ -\boldsymbol{x}_\lambda \end{bmatrix} \right\}}_{c(v_j)-1 \text{ vector(s)}}.$$

Note that,

$$Q\boldsymbol{x}_\lambda = \begin{bmatrix} 2 & -1 \\ -1 & 1 \end{bmatrix} \begin{bmatrix} \frac{-1}{2-\lambda} \\ -1 \end{bmatrix} = \begin{bmatrix} \frac{-\lambda}{2-\lambda} \\ \frac{\lambda-1}{2-\lambda} \end{bmatrix} = \lambda \begin{bmatrix} \frac{-1}{2-\lambda} \\ -1 \end{bmatrix} = \lambda \boldsymbol{x}_\lambda, \tag{12}$$

where the second equality from the right of (12) holds if $\lambda = \theta$ or θ^*. From this

it is easy to see that

$$B_j \boldsymbol{y}_\ell = \lambda \boldsymbol{y}_\ell, \quad \ell = 1, \ldots, c(v_j) - 1.$$

Hence, $\boldsymbol{y}_\ell$ is an eigenvector of B_j with eigenvalue λ for each $\ell = 1, \ldots, c(v_j) - 1$.

It is clear that $\boldsymbol{r}_j^\top \boldsymbol{y}_\ell = 0$ for all $\ell = 1, \ldots, c(v_j) - 1$ using the definition of both vectors. Hence we can construct our eigenvectors for $L(G)$ corresponding to the eigenvalue $\lambda = \theta$ or θ^* as

$$\boldsymbol{\phi}_{(\ell,j)} = \begin{bmatrix} \mathbf{0}_{2c(v_1)} \\ \vdots \\ \mathbf{0}_{2c(v_{j-1})} \\ \boldsymbol{y}_\ell \\ \mathbf{0}_{2c(v_{j+1})} \\ \vdots \\ \mathbf{0}_{2c(v_\kappa)} \\ \mathbf{0}_{n-\sum_{i=1}^{\kappa} 2c(v_i)} \end{bmatrix}, \tag{13}$$

for each $j = 1, \ldots, \kappa$ and $\ell = 1, \ldots, c(v_j) - 1$. It is clear that the multiplicity of θ accounted by the vectors of the form (13) is $\sum_{j=1}^{\kappa} (c(v_j) - 1)$, which is exactly equal to τ_{V_I}. The same argument also holds for θ^*. Therefore the inequality of (7) is achieved.

Finally, in order to show $m_G(\theta) = m_G(\theta^*)$, let us first recall that the characteristic polynomial of $L(G)$ is a monic polynomial of integer-valued coefficients. Moreover, the numbers θ and θ^* are the so-called *algebraic integers* in the field of $\mathbb{Q}\left[\sqrt{5}\right]$ [1, Chap. 13]. Combining these with the fact that the eigenvalues of $L(G)$ are nonnegative real numbers, thanks to the Galois theory [1, Chap. 16], we know that if θ is a root of such characteristic polynomial, then its "real conjugate" θ^* must also be a root and their multiplicities must be the same, i.e., $m_G(\theta) = m_G(\theta^*)$. □

We note that the eigenvectors constructed in (13) do not include the remaining eigenvectors of L, especially those related to the C_1, C_2, C_3, and C_4 portions.

We now present some examples below to demonstrate our Theorem 4.4.

Example 4.5 ($m_G(\theta) = m_G(\theta^*) = \tau_{V_I}$)**.** Figure 8 shows that $\tau_{V_I} = 3$. We can see this by observing the bordered rectangles encompassing the indicated vertices. Here, we have $v_i \in V_I$ with $c(v_i) = 2$ for each $i = 1, 2, 3$ in Figure 8. By comparison to the results displayed in Figure 6(b), we see that $m_G(\theta) = m_G(\theta^*) = 3 = \tau_{V_I}$.

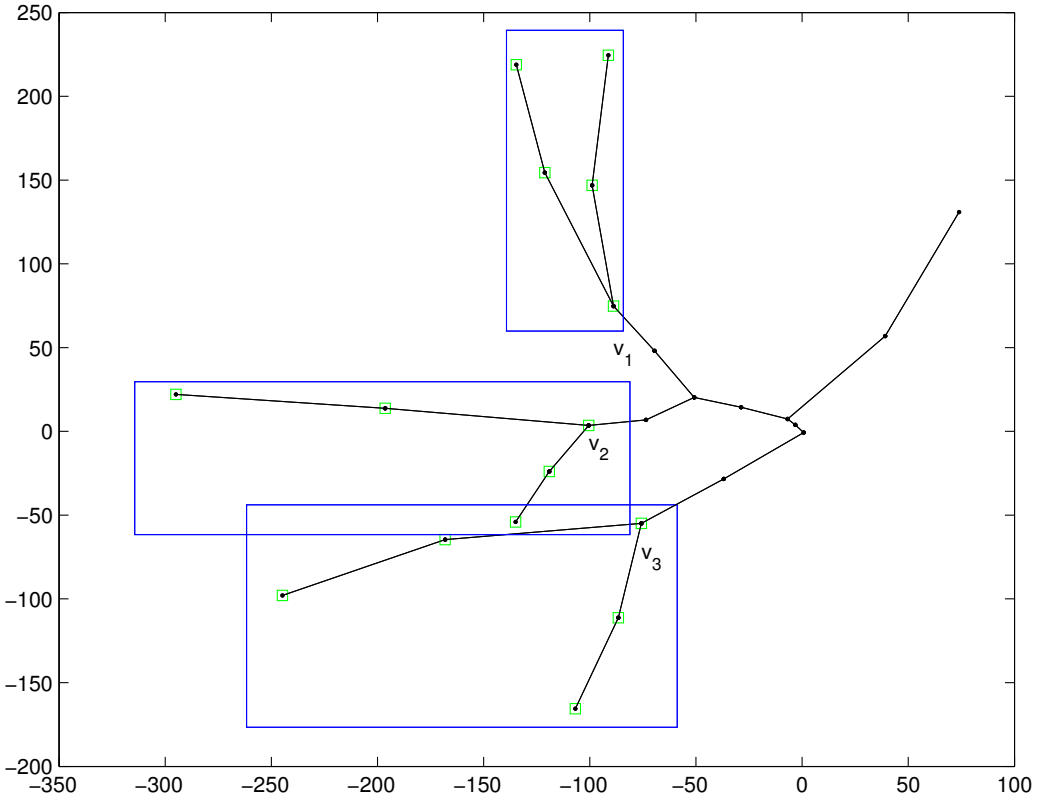

Figure 8: RGC #102 of Cluster 6 dendritic tree simplified. $v_i \in V_I$ for each $i = 1,2,3$ with $c(v_i) = 2$ for $i = 1,2,3$, hence $\tau_{V_I} = 3$.

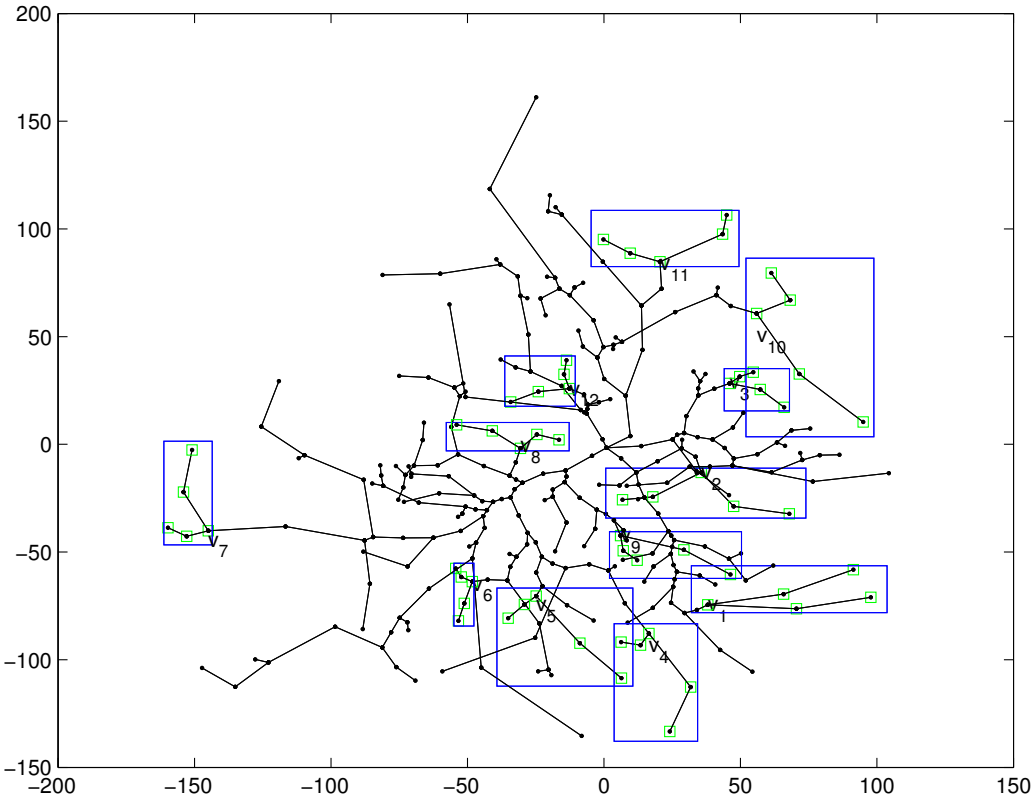

Figure 9: RGC #96 of Cluster 3 dendritic tree simplified. $\tau_{V_I} = 12$, yet $m_G(\theta) = m_G(\theta^*) = 13$. Vertices of interest are surrounded by green outlined squares and encompassed by a rectangle.

Example 4.6 ($m_G(\theta) = m_G(\theta^*) \gneqq \tau_{V_I}$)**.** Figure 9 shows an example where $13 = m_G(\theta) = m_G(\theta^*) \gneqq \tau_{V_I} = 12$. The rectangles in this figure indicates locations of vertices $v_i \in V_I$ for $i = 1, 2, \ldots, 12$, which contribute to τ_{V_I}.

5. Discussion

In this article, we introduced a tree simplification procedure that yielded the highly pronounced "eigenvalue plateaux" phenomenon in all of our simplified dendritic trees. We explained the reason of the occurrence of this phenomenon by splitting the vertex set V of a graph (more general than such simplified trees) into a set of mutually exclusive subsets, V_I, $V^I_{2\sim 1}$, V^I_1, and V_r followed by the explicit construction of eigenvectors corresponding to the multiple eigenvalues.

We now discuss a potential generalization to our Theorem 4.4. Recall the following theorem on the relationship between the pendant vertices and pendant neighbors:

Theorem 5.1 (Faria [5]; see also Merris [7])**.** *Let G be a graph, and let $p(G)$ and $q(G)$ be the number of pendant vertices and pendant neighbors in G, respectively. Then,*

$$p(G) - q(G) \leq m_G(1).$$

This inequality was used to derive a spectral feature for clustering dendritic trees in [9]. In this article, if we refer to the vertices in V_I as *pendant P_2 neighbors* and the vertices in the set $V_{2\sim 1}^I$ as *pendant P_2 vertices*, with $q_2(G)$ and $p_2(G)$ as their cardinalities, respectively, then it is clear that $p_2(G) = \left|V_{2\sim 1}^I\right| = \sum_{v\in V_I} c(v)$, $q_2(G) = |V_I| = \kappa$. Hence, Theorem 4.4 can be rewritten as

$$p_2(G) - q_2(G) \leq m_G(\theta) = m_G(\theta^*).$$

More generally, let us define the notion of a *pendant P_j vertex* and a *pendant P_j neighbor*. A vertex v in a graph $G(V,E)$ with $|V| = n$ is said to be a pendant P_j vertex ($1 \leq j \leq n$) if the following conditions are satisfied: 1) v is a trivial vertex; 2) v is adjacent to a nontrivial vertex u of degree greater than two; and 3) there is a pendant vertex $w \in V$ such that u and w form a neighboring pair of nontrivial vertices with a path of length j. A vertex $u \in G(V,E)$ is said to be a pendant P_j neighbor if u is a nontrivial vertex with degree greater than two and is adjacent to a pendant P_j vertex. We then have the following:

Conjecture 5.2. Let $G(V,E)$ be a simple, connected, undirected, and unweighted graph with $|V| = n$. Let $1 \leq j \leq n$, and let $p_j(G)$, $q_j(G)$ be the number of pendant P_j vertices and the number of pendant P_j neighbors, respectively. Then,

$$p_j(G) - q_j(G) \leq m_G(\lambda_s(G)),$$

holds for some $s \in \{0,\ldots,n-1\}$.

This conjecture is certainly true if $G(V,E) = S(k.m)$ where $1 \leq j \leq m$. This is because we can easily show from the definitions:

$$p_j(G) = \begin{cases} 0 & \text{if } 1 \leq j < m; \\ k & \text{if } j = m \end{cases} \quad \text{and} \quad q_j(G) = \begin{cases} 0 & \text{if } 1 \leq j < m; \\ 1 & \text{if } j = m \end{cases}$$

imply

$$p_j(G) - q_j(G) = \begin{cases} 0 & \text{if } 1 \le j < m; \\ k-1 & \text{if } j = m. \end{cases}$$

Since $m_G(\lambda_s(G)) \ge 0$ for every $s \in \{0,1,\ldots,n-1\}$, the former case of $p_j(G) - q_j(G) = 0 \le m_G(\lambda_s(G))$ is certainly true. If $j = m$, then there are m eigenvalues with multiplicity $k-1$ as Lemma 3.1 of Das [4] shows. Hence, $p_j(G) - q_j(G) = k-1 \le m_G(\lambda_s(G))$ also holds for certain $s \in \{0,1,\ldots,n-1\}$.

Acknowledgments

N. S. would like to thank Prof. Monica Vazirani of UC Davis for explaining the basics of the roots of a monic polynomial with integer coefficients. This research was partially supported by the following grants from the Office of Naval Research: N00014-09-1-0041; N00014-09-1-0318; N00014-12-1-0177 as well as the National Science Foundation: DMS-0636297; DMS-1418779.

References

[1] M. Artin, Algebra, 2nd Edition, Prentice Hall, 2011.

[2] W. Chen, N. Saito, E. Woei, Clustering dendritic patterns via weighted graph Laplacian eigenvalues, Tech. rep., Dept. Math., Univ. California, Davis, in preparation (2015).

[3] J. Coombs, D. van der List, G.-Y. Wang, L. M. Chalupa, Morphological properties of mouse retinal ganglion cells, Neuroscience 140 (2006) 123–136.

[4] K. C. Das, Some spectral properties of the Laplacian matrix of starlike trees, Italian Journal Pure and Applied Mathematics 21 (2007) 197–210.

[5] I. Faria, Permanental roots and the star degree of a graph, Linear Algebra Applications 64 (1985) 255–265.

[6] C. Godsil, G. Royle, Algebraic Graph Theory, Vol. 207 of Graduate Texts in Mathematics, Springer, New York, 2001.

[7] R. Merris, Laplacian matrices of graphs: A survey, Linear Algebra Applications 197/198 (1994) 143–176.

[8] Y. Nakatsukasa, N. Saito, E. Woei, Mysteries around graph Laplacian eigenvalue 4, Linear Algebra and Its Application 438 (8) (2013) 3231–3246.

[9] N. Saito, E. Woei, Analysis of neuronal dendrite patterns using eigenvalues of graph Laplacians, JSIAM Letters 1 (2009) 13–16, invited paper.

[10] N. Saito, E. Woei, On the phase transition phenomenon of graph Laplacian eigenfunctions on trees, RIMS Kôkyûroku 1743 (2011) 77–90.

[11] G. Strang, The discrete cosine transform, SIAM Review 41 (1999) 135–147.

[12] G. Stuart, N. Spruston, M. Häusser, Dendrites, 2nd Edition, Oxford Univ. Press, 2008.

[13] E. Woei, Characterization and clustering of dendritic trees using morphological features extracted by graph spectra, Ph.D. thesis, University of California, Davis (December 2012).